

Predicted Liquefaction of East Bay Fills During a Repeat of the 1906 San Francisco Earthquake

Thomas L. Holzer,^{a)} M.EERI, J. Luke Blair,^{a)} Thomas E. Noce,^{a)}
and Michael J. Bennett^{a)}

Predicted conditional probabilities of surface manifestations of liquefaction during a repeat of the 1906 San Francisco (M7.8) earthquake range from 0.54 to 0.79 in the area underlain by the sandy artificial fills along the eastern shore of San Francisco Bay near Oakland, California. Despite widespread liquefaction in 1906 of sandy fills in San Francisco, most of the East Bay fills were emplaced after 1906 without soil improvement to increase their liquefaction resistance. They have yet to be shaken strongly. Probabilities are based on the liquefaction potential index computed from 82 CPT soundings using median (50th percentile) estimates of PGA based on a ground-motion prediction equation. Shaking estimates consider both distance from the San Andreas Fault and local site conditions. The high probabilities indicate extensive and damaging liquefaction will occur in East Bay fills during the next $M \sim 7.8$ earthquake on the northern San Andreas Fault.

[DOI: 10.1193/1.2188018]

INTRODUCTION

Some of the most spectacular examples of damage during the 1906 San Francisco, California, M7.8 earthquake on the San Andreas Fault (USGS 2003) were caused by liquefaction of loose sandy artificial fills in areas of made ground in San Francisco (Youd and Hoose 1978). In addition to settlements and bearing capacity failures beneath buildings, large liquefaction-induced ground displacements broke both water transmission and distribution lines that contributed to the inability to suppress the post-earthquake fire that consumed 490 city blocks (11.5 km²) in San Francisco. Despite the poor performance of these fills in 1906, extensive new fills continued to be emplaced around the margins of San Francisco Bay, often with sandy soils and emplacement techniques similar to those used in pre-1906 fills. Thus liquefaction of sandy artificial fills along the San Francisco waterfront in 1906 is an ominous foreboding of the liquefaction potential of many of the post-1906 fills during the next large earthquake on the northern San Andreas Fault.

This paper presents predictions of liquefaction of the large sandy fills along the Alameda, Berkeley, Emeryville, and Oakland waterfronts, here referred to as the East Bay fills, during a repeat of the 1906 M7.8 earthquake (Figures 1 and 2). Most of these

^{a)} U.S. Geological Survey, 345 Middlefield Road, Menlo Park, CA 94025

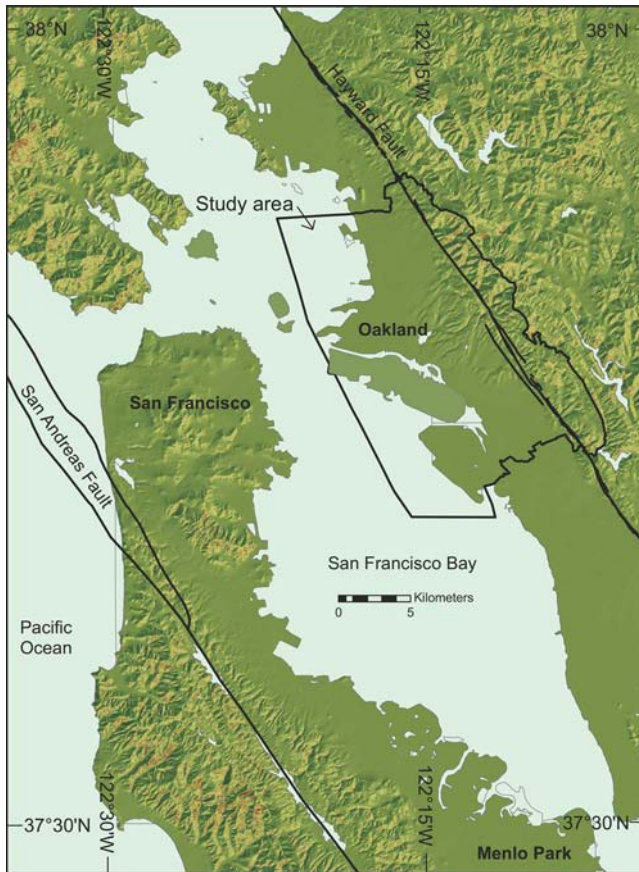


Figure 1. Map of San Francisco Bay area, California, East Bay fill study area, and parts of the San Andreas and Hayward Faults. San Andreas Fault traces from R. C. Jachens (written comm. 2005). The calculated distance from the San Andreas Fault was the average distance to the two traces. The 1906 M7.8 earthquake ruptured a 430-km-long segment of the San Andreas Fault (WGCEP 2003).

fills were emplaced after 1906, and thus were not subjected to shaking from the 1906 earthquake. Owing to a lack of awareness of liquefaction as a seismic hazard, these fills typically were not improved when they were emplaced and are similar to many of the pre-1906 fills in San Francisco. Thus, in general, they can be expected to perform poorly when shaken strongly by future large earthquakes on the San Andreas Fault as well as other Bay Area faults. It should be noted that subsequent recognition of liquefaction as a hazard has prompted local soil improvements (or liquefaction-resistant construction) at some sites. The predictions here do not apply to these sites. The predictive approach follows the methodology that was developed and applied to produce liquefaction potential maps of the greater Oakland area for an M7.1 Hayward Fault earthquake (Holzer et al. 2002, 2006). In that study, it was estimated that approximately three-quarters of the area

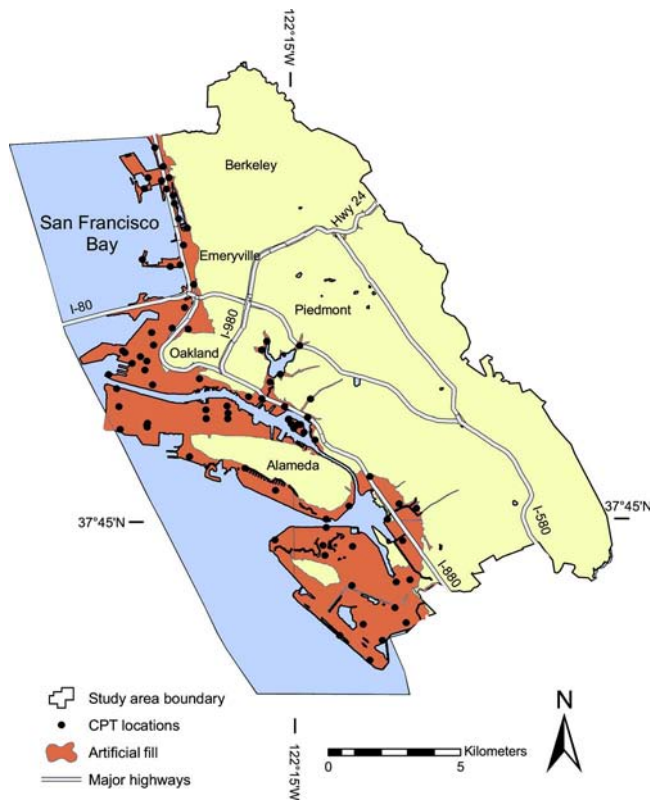


Figure 2. Study area with East Bay artificial fills and locations of CPT soundings. See Figure 1 for location of study area. Fill area from Helley and Graymer (1997).

underlain by the East Bay fills would liquefy during the scenario earthquake. The methodology used in both that and the present study relies on the liquefaction potential index (LPI) to compute conditional probabilities of surface manifestations of liquefaction. We conclude that significant portions of the artificial fills along the Oakland and Alameda waterfronts will liquefy and disrupt buried and surface facilities when the next 1906-type earthquake occurs on the San Andreas Fault.

II. HISTORY OF ARTIFICIAL FILLS—SAN FRANCISCO BAY

Since 1847, tens of millions of cubic meters of fills have been placed into San Francisco Bay proper to reclaim more than 245 km² of marshland and tidal and submerged land (USDC 1959). Most of this land was reclaimed after 1906. The largest of the post-1906 sandy fills are Treasure Island, the waterfronts of Oakland and Alameda, and the Marina District in San Francisco. The focus of the present investigation is the Oakland and Alameda fills, which are the largest of these three fills. They underlie an area of 57 km². While the history of the Oakland and Alameda fills, which began in 1879, is

complex, most of the fill was emplaced after 1906, often by hydraulic dredging of sand (Rogers and Figuers 1991). The largest fill, six million cubic meters, was placed between January 1941 and June 1942 to create the former Alameda Naval Air Station and Oakland Army Base.

With the exception of the 1989 Loma Prieta (M6.9) earthquake, the land underlain by post-1906 fills has not been subjected to strong shaking. Because of the similarity of the post-1906 fills to the pre-1906 fills in San Francisco, the liquefaction of sandy fills in 1906 bodes poorly for the performance of the post-1906 sandy fills in future earthquakes. Although ground shaking from the Loma Prieta earthquake was modest (peak ground acceleration ≈ 0.2 g) in areas underlain by East Bay fills, liquefaction was widespread (Holzer 1998a). Treasure Island, the Port of Oakland, Oakland airport, the San Francisco-Oakland Bay Bridge toll plaza, Alameda Naval Air Station, and Bay Farm Island all experienced significant liquefaction damage. Holzer (1998b, Table 1) estimated that losses caused by liquefaction in these areas equaled approximately \$54 million (\$84 million in 2005 dollars).

METHODOLOGY

In the investigation described in this paper, the spatial distribution of the conditional probability of surface manifestations of liquefaction in the area underlain by artificial fill was predicted for a repeat of a 1906 M7.8 earthquake on the northern San Andreas Fault. Conditional probabilities were computed in two steps. First, the spatial distribution of peak ground acceleration (PGA) for a M7.8 earthquake on the San Andreas Fault was estimated with a ground-motion prediction (attenuation) equation. Values were computed for a grid with a 50-m nodal spacing. Second, 82 cone penetration test (CPT) soundings conducted in the East Bay fills by the USGS were used to develop a relation between the probability of surface manifestations of liquefaction and PGA for a M7.8 earthquake (CPT data are available at <http://quake.usgs.gov/prepare/cpt/>). As will be discussed, liquefaction probabilities are based on cumulative frequency distributions of the liquefaction potential index (LPI). Thus, by predicting values of PGA at nodes within a grid for a M7.8 San Andreas Fault earthquake, the conditional probability of liquefaction could be estimated at the same nodes and contoured to produce a map of liquefaction probabilities.

PEAK GROUND ACCELERATION

PGA was estimated with the ground-motion prediction equation (GMPE) of Boore et al. (1997) and Boore (2005) for a vertical strike-slip fault. This GMPE is based on a statistical regression of recordings of strong ground motion data in Western North America. The estimated PGA is the geometric mean of the maximum two horizontal components of PGA, which for the earthquake scenario here is about 10% less than the predicted maximum value of either component. Predicted PGA versus distance from the San Andreas Fault for an M7.8 earthquake and an average East Bay fill site condition, $V_{S30} = 180$ m/s, are shown in Figure 3. V_{S30} is the average shear-wave velocity to a depth of 30 m, and is computed by dividing 30 m by the travel time of a vertically propagating shear wave. Figure 3 also shows PGA predicted with GMPEs proposed by

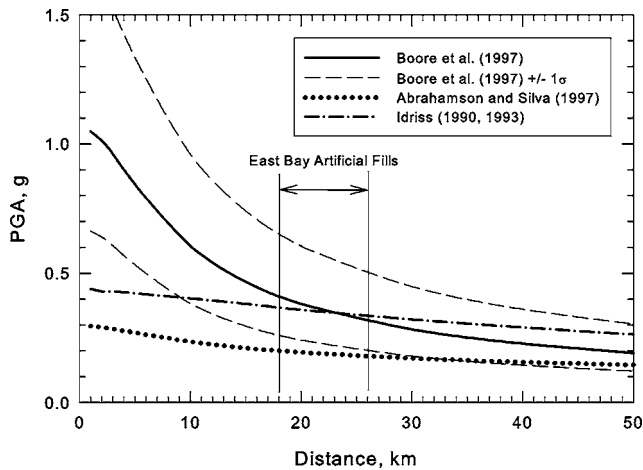


Figure 3. Predicted PGA as a function of distance from the San Andreas Fault for M7.8 earthquake. Site conditions are Boore et al. (1997), $V_{S30}=180$ m/s (median and $\pm 1\sigma$); Abrahamson and Silva (1997), $V_{S30}=180$ m/s (as modified by Choi and Stewart, 2005); and Idriss (1990, 1993), “soft soil.”

Abrahamson and Silva (1997) and Idriss (1990, 1993). To predict PGA for a $V_{S30}=180$ m/s site condition with Abrahamson and Silva (1997), the amplification factors proposed by Choi and Stewart (2005, Equation 5 and Table A1) were applied to PGA predicted for rock sites. PGA values for Idriss were computed by first using his GMPE for rock (Idriss 1993) and then using Idriss (1990, Figure 11) to modify the PGA to a soft soil condition, which corresponds to $V_{S30}\approx 180$ m/s. The small variation of PGA with distance predicted by Abrahamson and Silva and Idriss is attributable to nonlinear soil behavior at large PGA and amplification at small PGA.

Predictions by the other two GMPEs are within approximately one standard deviation (σ) of median values predicted with Boore et al. (1997) at the distance interval corresponding to the minimum and maximum distances of the East Bay fills from the San Andreas Fault. In fact, agreement is very good between Boore et al. (1997) and Idriss (1990, 1993) for a soft soil condition. Predictions with Abrahamson and Silva (1997) as modified by Choi and Stewart (2005) fall slightly below the 16th percentile (median -1σ) PGA predicted with Boore et al. (1997). The lower predicted PGA values are caused by a nonlinear site term, whereas Boore et al. (1997) use a linear site term.

The principal reason for selecting the Boore et al. (1997) GMPE was that it directly considers V_{S30} . This allows local site conditions, which were mapped in a previous investigation (Holzer et al. 2005a), to be incorporated into the predictions of ground motion. Consideration of local site effects is important in the study area because the artificial fill is mostly underlain by normally consolidated soft mud that was deposited in San Francisco Bay. The mud, which is informally known as younger Bay mud, is a Holocene estuarine silty clay. Shear wave velocity of the mud is depth dependent, although

the average is approximately 118 m/s (Holzer et al. 2005b). Such soft soils commonly amplify local ground shaking at weaker levels of shaking and may de-amplify shaking at stronger levels (Joyner and Boore 1988). Lateral variations of V_{S30} in the study area can be abrupt because the mud was deposited on an eroded surface with significant relief. The mud may locally attain thicknesses greater than 30 m. It is thickest in the study area where it fills channels that were incised by streams during Pleistocene periods of low sea level (see Holzer et al. 2005a, Figure 5a).

Predicted values of PGA cannot be directly compared to 1906 San Francisco earthquake shaking because the event predated strong ground-motion recording instrumentation. Thus 1906 ground motion must be inferred from other observations. Recently, Boatwright and Bundock (2005) re-evaluated shaking intensity for the 1906 earthquake. They inferred that Modified Mercalli Intensity (MMI) for NEHRP D/E site classes, which is the prevalent site condition beneath the fills (Holzer et al. 2005b), was approximately VIII at 18–26 km from the fault (J. Boatwright, written comm., 2005). For the Oakland waterfront, they inferred MMI VIII 1/2. According to Wald et al. (1999), MMI VIII corresponds to $0.32 \text{ g} < \text{PGA} < 0.65 \text{ g}$. The predicted range of PGA in the study area based on $V_{S30}=180 \text{ m/s}$, 0.31 to 0.41 g (Figure 3), is within the lower part of the range inferred from MMI. Because the next $M \sim 7.8$ earthquake on the northern San Andreas Fault may not have the same seismogenic rupture as that in 1906, it may not generate similar ground motion in Oakland. Accordingly, 16th and 84th percentile values of PGA were computed in addition to median values. These two percentiles, which are based on $\pm 1\sigma$'s (Boore et al. 1997), define the likely range of PGA in the East Bay to be expected during future $M \sim 7.8$ earthquakes on the northern San Andreas Fault.

LIQUEFACTION PROBABILITY

The conditional probability of liquefaction was inferred from cumulative frequency distributions of LPI computed with the 82 CPT soundings that were conducted in the East Bay fills. LPI was originally proposed to estimate the potential for liquefaction to cause foundation damage (Iwasaki et al. 1978). The index weighs factors of safety and thickness of potentially liquefiable layers according to depth. It assumes that the severity of liquefaction is proportional to

1. cumulative thickness of the liquefied layers;
2. proximity of liquefied layers to the surface; and
3. amount by which the factor safety (FS) is less than 1.0, where FS is the ratio of soil capacity to resist liquefaction to seismic demand imposed by the earthquake. Iwasaki et al. (1978) defined the index as

$$LPI = \int_0^{20m} Fw(z) dz \quad (1)$$

where

$$F = 1 - FS \quad \text{for } FS \leq 1 \quad (2a)$$

$$F = 0 \quad \text{for } FS > 1 \quad (2b)$$

$$w(z) = 10 - 0.5z, \quad \text{where } z \text{ is the depth in meters.} \quad (2c)$$

The weighting factor, $w(z)$, proposed by Iwasaki et al. (1978) ranges from one at the surface to zero at 20 m. For the present investigation, we used the FS as defined in the Seed-Idriss simplified procedure (Seed and Idriss 1971, Seed et al. 1985, Youd et al. 2001) and as modified for the CPT by Robertson and Wride (1997). For the purposes of hazard mapping, the advantage of LPI compared to the simplified procedure is that it predicts the liquefaction potential of the whole soil column. The simplified procedure just predicts the liquefaction potential of a soil element. By combining all of the factors of safety from a sounding into a single value, LPI provides a spatially distributed parameter if multiple soundings are conducted in a deposit.

Iwasaki et al. (1982) and Toprak and Holzer (2003) have independently determined the significance of LPI values. Both groups compiled case histories that correlated LPI with the observed severity of liquefaction. Iwasaki et al. (1982) concluded that severe liquefaction is likely at sites with $LPI > 15$ and that severe liquefaction is unlikely at sites with $LPI < 5$. Their computations of LPI relied on blow counts from standard penetration tests and a FS defined by Iwasaki et al. (1982). Toprak and Holzer (2003) computed LPI values from CPT soundings at sites with surface manifestations of liquefaction during the 1989 Loma Prieta, California, earthquake, and concluded that sand boils typically occur where $LPI \geq 5$. Their threshold is based on median LPI values. Lower and upper quartiles were 3 and 10 for sand boils. Toprak and Holzer (2003) used the same methodology as was used in this investigation to calculate LPI.

To calculate conditional probabilities of surface manifestations of liquefaction in the East Bay fills, LPI values were computed for each of the 82 CPT soundings assuming a water table depth of 1.5 m. Although we computed LPI values for the whole depth penetrated by the sounding, most of the liquefaction potential in each of the soundings is in the artificial fill. For the application here, LPI values were computed for each sounding for a M7.8 earthquake and range of PGA from 0 to 0.6 g. Cumulative frequency distributions of LPI were then compiled for each PGA using the same 82 soundings for each distribution (Figure 4a). In other words, each curve in Figure 4a is based on LPI values computed with the same 82 soundings at a given PGA value. If the spacing of the CPT soundings is approximately uniform in the area of artificial fill and one assumes that the fill is statistically homogeneous, the cumulative frequency at $LPI=5$ can be interpreted as the probability that surface manifestations of liquefaction will occur at an arbitrary location in the fill when shaken at the specified PGA. This frequency also can be interpreted as a percentage of the total surface area that will exhibit surface manifestations of liquefaction. To illustrate with an example, consider the frequency distribution in Figure 4a for $PGA=0.20$ g, where 35% of the soundings have $LPI \geq 5$. If an arbitrary location is shaken at $PGA=0.20$ g, there is a 0.35 probability of surface manifestations of liquefaction. Alternatively, if the whole area is shaken at 0.20 g, 35% of the land area is predicted to exhibit surface manifestations of liquefaction.

By plotting the cumulative frequency at $LPI=5$ from each distribution shown in Figure 4a, the probability of surface manifestation of liquefaction in the artificial fill as a function of PGA can be estimated for a M7.8 earthquake (Figure 4b). Liquefaction prob-

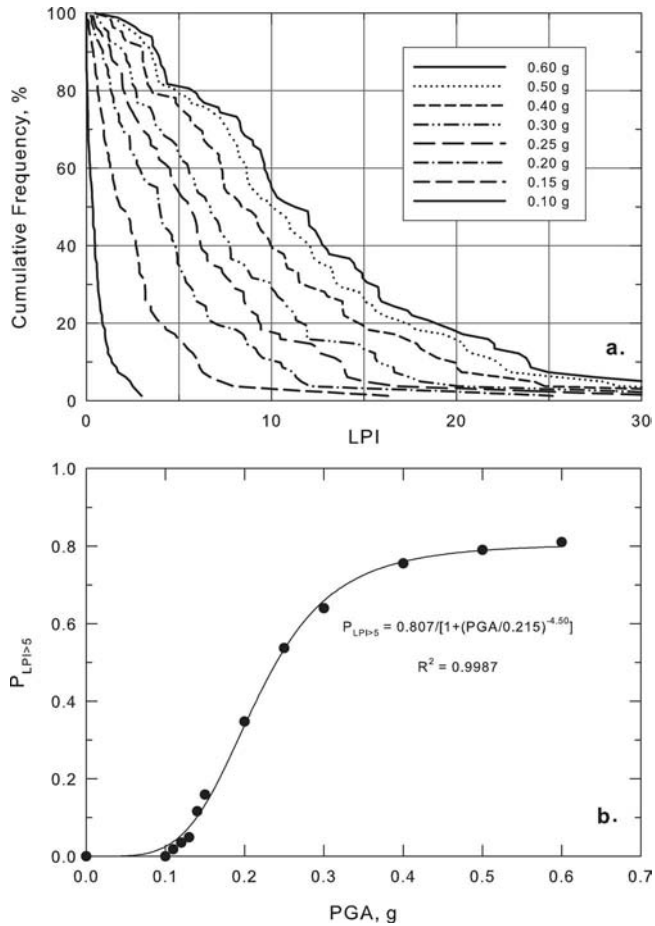


Figure 4. (a) Cumulative frequency distributions of LPI for East Bay artificial fills for M7.8 earthquake and different PGA values; (b) Probability of surface manifestations of liquefaction versus PGA (M=7.8) for East Bay fills determined from LPI=5 in (a). Probabilities were fitted with a 4 parameter logistic curve. Cumulative frequency distributions are not shown in (a) for PGA ranging from 0.11 to 0.14 g.

ability of the East Bay fills for a M7.8 earthquake increases rapidly with PGA from approximately 0.14 to 0.30 g, at which level the rate of increase of probability decreases. The probability at large PGA approaches an asymptote of approximately 0.8.

LIQUEFACTION PREDICTIONS

Median PGA values predicted for the East Bay fills for a M7.8 earthquake on the northern San Andreas Fault are mapped in Figure 5. Predicted PGA ranges from 0.25 to 0.54 g. The map was produced by contouring PGA values computed at nodes in a 50-m interval grid, where each nodal PGA value was predicted with the Boore et al. (1997)

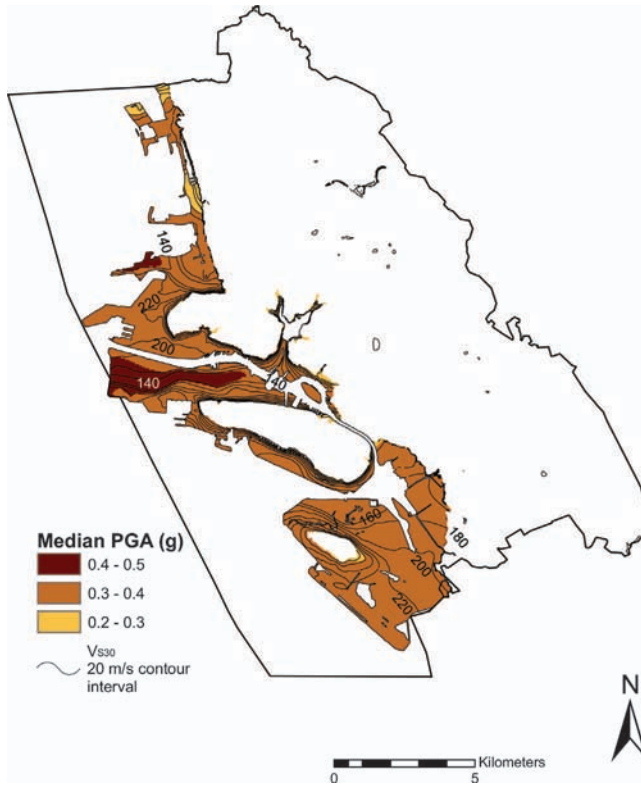


Figure 5. Median PGA in area of East Bay fills for M7.8 earthquake on northern San Andreas Fault predicted with Boore et al. (1997). Contours show V_{S30} values from Holzer et al. (2005b) that were used to predict PGA with Boore et al. (1997). *In color:* see plates following p. S68.

GMPE. Although the distance of the study area from the San Andreas Fault ranges from 18 to 26 km, variations of distance account for only approximately 35% (0.1 g) of the total variation of PGA. The remainder of the variation is attributable to local site conditions. Contours of V_{S30} values used to predict the spatial variation of ground motion are shown in Figure 5. Note that the largest PGA values are associated with the buried channels (low V_{S30}) that were discussed previously. Although not shown here, maps of 16th and 84th percentile PGA were also computed with the median $\pm 1\sigma$ PGA of Boore et al. (1997) (see dashed curves in Figure 3). These scenarios reflect the range of PGA motion that is likely for alternative seismogenic ruptures of the northern San Andreas Fault. The pattern of variation in PGA for the maps of 16th and 84th percentile PGA is similar to that in Figure 5, but absolute values differ. Values vary from 0.40 to 0.85 g for 84th percentile (median $+1\sigma$) and from 0.16 to 0.34 g for 16th percentile (median -1σ) PGA.

Conditional probabilities of surface manifestations of liquefaction in the East Bay fills for median (50th percentile) PGA are shown in Figure 6. The map was produced by using the relation between liquefaction probability and PGA in Figure 4b to associate

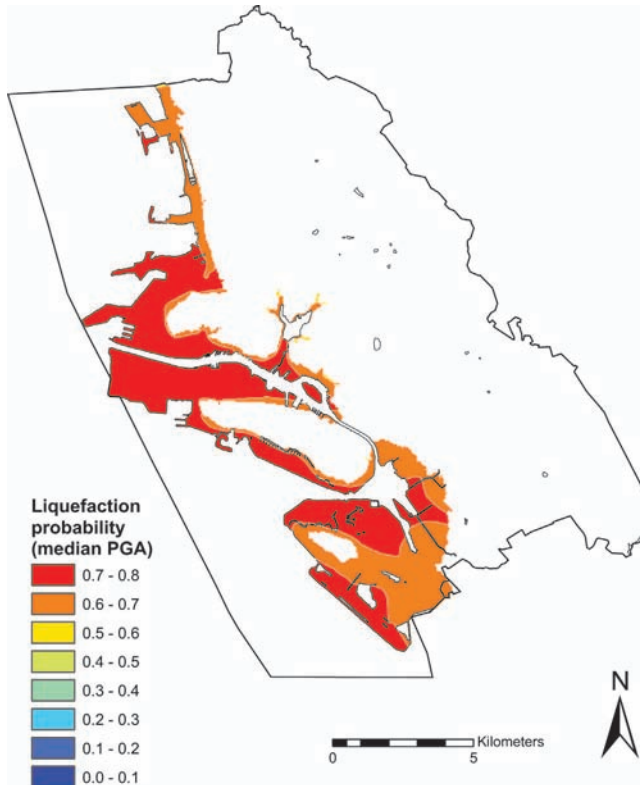


Figure 6. Predicted probabilities of surface manifestations of liquefaction for M7.8 earthquake on the San Andreas Fault based on median PGA predicted with Boore et al. (1997). *In color:* see plates following p. S68.

liquefaction probability with PGA in Figure 5. Probabilities range from 0.54 to 0.79. Probabilities are greater than 0.70 in more than 50% of the fill area.

Conditional probabilities of surface manifestations of liquefaction for 16th and 84th percentile PGA are shown in Figures 7 and 8, respectively. Even for 16th percentile PGA, the liquefaction probability is greater than 0.50 in 18% of the area underlain by fill. This scenario also has the greatest range of liquefaction probabilities, 0.16 to 0.71. Probabilities are highest in areas where V_{S30} is lowest, the buried stream channels. The effect of the buried channels is most evident along the western end of Alameda Island, the large island in the study area, at the former Alameda Naval Air Station. Probabilities for the 84th percentile PGA are only slightly greater than those for the median PGA, exceeding 0.70 in all of the study area. The high liquefaction probability results from $PGA > 0.60$ g throughout most of the study area. It also should be noted that ground motions estimated by Abrahamson and Silva (1997) as modified by Choi and Stewart (2005) would approximately predict the probabilities in Figure 7 because they correspond to the 16th percentile PGA.

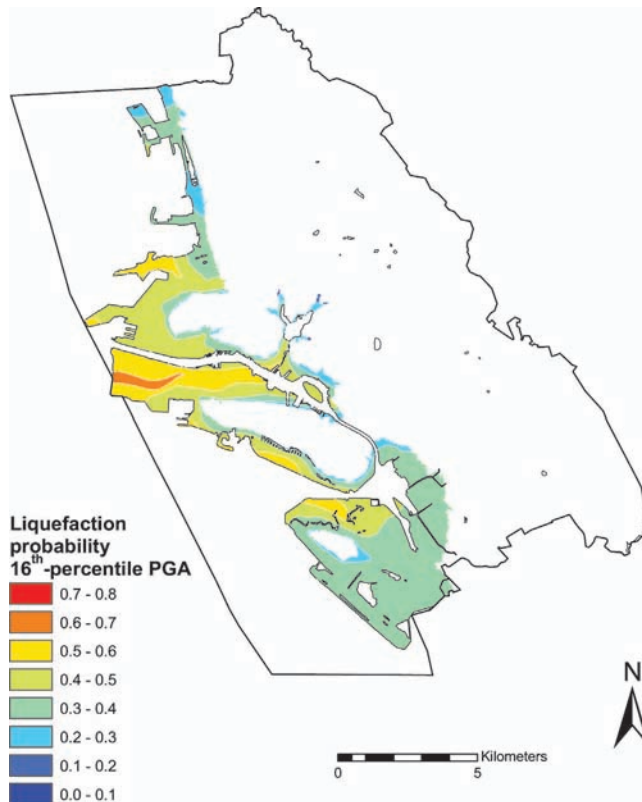


Figure 7. Predicted probabilities of surface manifestations of liquefaction for M7.8 earthquake on the San Andreas Fault based on 16th percentile (median -1σ) PGA predicted with Boore et al. (1997). Predictions do not apply to local areas where soil has been improved. *In color:* see plates following p. S68.

DISCUSSION

PGA in the East Bay for a recurrence of the 1906 San Francisco (M7.8) earthquake was estimated in this investigation with median ground motions based on the Boore et al. (1997) GMPE. Regardless of how well their median PGA characterizes 1906 ground motion, the next $M \sim 7.8$ earthquake on the northern San Andreas Fault may not necessarily involve a repetition of the seismogenic rupture that occurred in 1906. If not, then ground motions in the Oakland area may differ substantially from those that were generated in 1906. This possibility prompted us to compute three maps of the conditional probability of liquefaction (Figures 6–8) based on alternative ground motion scenarios: median, 16th and 84th percentile. Despite the large range of PGA predictions for these scenarios, 0.16 to 0.85 g, significant liquefaction in the area underlain by fill is predicted for all three scenarios.

Although we predicted only the probability and not the consequences of liquefaction

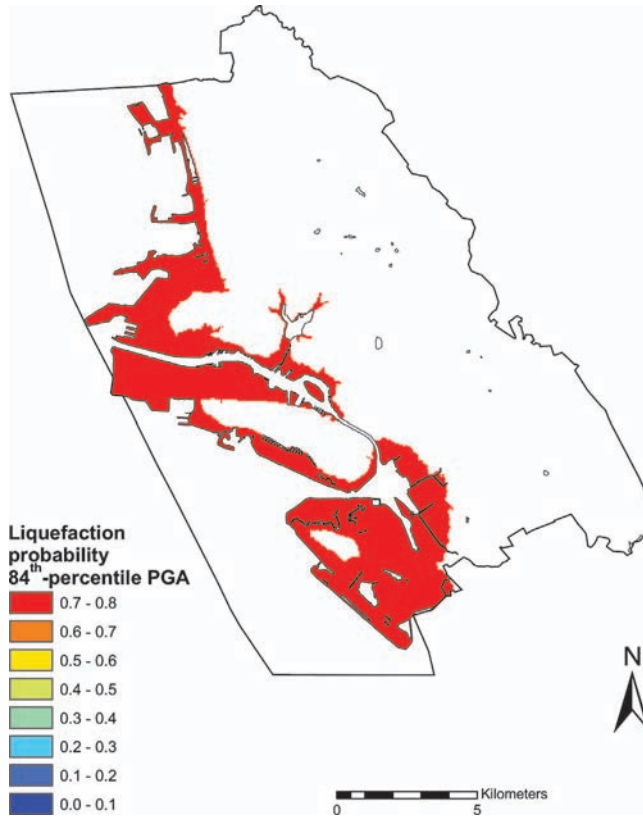


Figure 8. Predicted probabilities of surface manifestations of liquefaction for M7.8 earthquake on the San Andreas Fault based on 84th percentile (median +1 σ) PGA predicted with Boore et al. (1997). Predictions do not apply to local areas where soil has been improved. *In color:* see plates following p. S68.

of East Bay fills, this liquefaction can be expected to cause extensive damage because of the ground deformation—lateral spreading, ground settlements, bearing capacity failures, and ground oscillation—that typically accompanies widespread liquefaction. This ground deformation may damage quay walls, buried utilities, bridges, roadways, airport runways, and buildings that are not liquefaction resistant. For example, Holzer (1998b) estimated that liquefaction during the 1989 Loma Prieta M6.9 earthquake, which affected only a small portion of the East Bay fills in the study area, nevertheless caused \$49.8 million (\$77.6 million in 2005 dollars) of damage. Perhaps an even better analog because of their proximity to the seismic source zone is the response of artificial fills is the 1995 Hyogoken-Nanbu M6.9 earthquake. This earthquake caused widespread liquefaction of artificial fills at Kobe, Japan, and serious damage to lifelines, foundations, and bridge piles (Hamada and Wakamatsu 1996). As a result, approximately 95% of the shipping berths in the port of Kobe were inoperable after the earthquake.

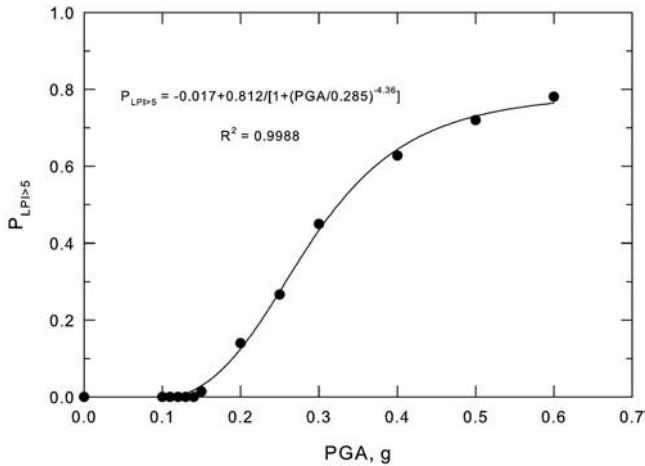


Figure 9. Predicted probability of surface manifestations of liquefaction in East Bay artificial fills versus PGA for a M6.9 earthquake.

Although our methodology and resulting predictions ultimately will be tested when the East Bay fills are shaken strongly by a suitable earthquake, the experience with the Hyogoken-Nanbu and Loma Prieta earthquakes provide credence to them. Hamada et al. (1995) conducted detailed mapping of surface effects from extensive liquefaction of the 27 km² of land underlain by sandy artificial fill in Osaka Bay near Kobe, Japan, after the Hyogoken-Nanbu earthquake. The earthquake, which initiated on the Nojima Fault and ruptured directly beneath Kobe, shook the fills strongly with near-field ground motion. PGA recorded on the fill exceeded 0.5 g (see Hamada et al. 1995, Figure 1.2). Maps of many of the artificial islands indicate that approximately 70–80% of the land in areas where soil had not been improved was covered by vented sand (see Hamada et al. 1995, Figure 2.3).

The Loma Prieta earthquake tests, albeit modestly, the predictive capability of the methodology in the study area. Approximately 13% of the area underlain by artificial fill showed surface manifestations of liquefaction as measured from 1:100,000-scale maps by Tinsley et al. (1998). To compare observed and predicted liquefaction in 1989, an estimate of the ground motion is required. Only two recordings of ground motion during the 1989 earthquake are available at sites underlain by fill and younger Bay mud in or near the study area. Mean PGAs recorded at Treasure Island and Oakland Outer Harbor Wharf, respectively, were 0.14 and 0.28 g (Brady and Shakal 1998), which suggests $PGA \approx 0.2$ g. To predict the area with surface manifestations of liquefaction, we computed cumulative frequency distributions for a M6.9 earthquake and generated a probability curve as a function of PGA in a manner similar to that which was done for the 1906 earthquake scenario. The resulting probability curve is shown in Figure 9. Based on a $PGA=0.2$ g, approximately 14% of the fill area is predicted to show surface manifestations of liquefaction. This PGA, incidentally, corresponds to a 95th percentile (me-

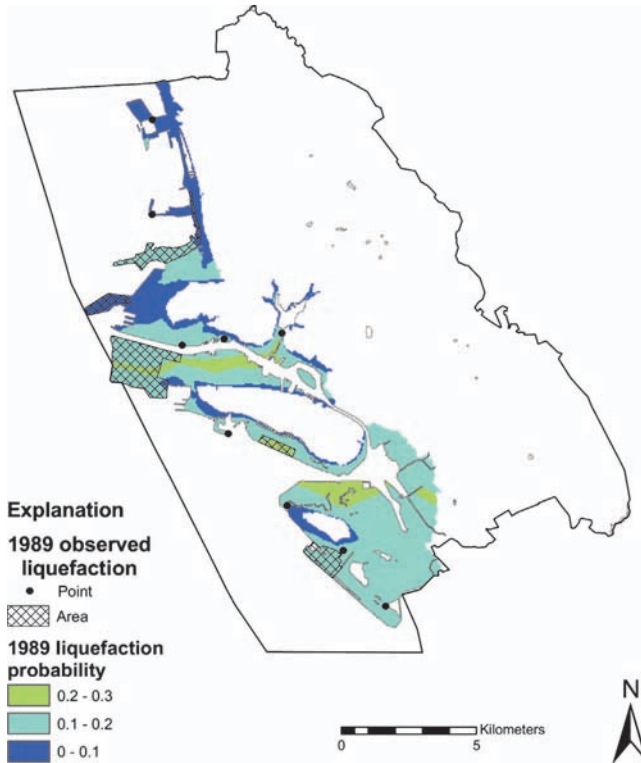


Figure 10. Map of probability of surface manifestations of liquefaction for 1989 Loma Prieta (M6.9) earthquake and locations of liquefaction mapped by Tinsley et al. (1998). *In color:* see plates following p. S68.

dian $+1.6\sigma$) PGA when compared to predictions with Boore et al. (1997) for an M6.9 earthquake on the fault segment that ruptured during the Loma Prieta earthquake.

In addition to predicting the size of the liquefaction area, locations of liquefaction in 1989 were plotted on a map of liquefaction probabilities (Figure 10). The conditional probabilities were computed with Figure 9 and PGAs predicted with Boore et al. (1997) for a M6.9 earthquake using their GMPE for 95th percentile (median $+1.6\sigma$) PGA. Three of the five liquefaction areas are in areas of higher probability. Locations of some of the 1989 liquefaction in areas of lower probability may be in part a manifestation of our assumption that the fills are statistically spatially homogenous. In fact, East Bay fills were emplaced over an 85-year period using a variety of techniques—land tipping and dredging—and source materials. Thus, on a local scale, variations in liquefaction susceptibility are to be expected. In addition, fill thickness, which has a strong correlation with LPI, ranges from zero along the old shore line to more than 10 m near the western margin of the fill (Holzer et al. 2005a, Figure 5b). This suggests that for regional map-

ping of liquefaction hazard, the interpretation of the cumulative frequency at $LPI=5$ as a percent area may be superior to the site-specific probability interpretation.

Finally, the dynamic response of the younger Bay mud at large PGA is an important consideration for ground motion estimation. Nonlinear soil behavior may reduce PGA below values predicted by the Boore et al. (1997) GMPE, which assumes the soil responds linearly to the level of shaking. Ironically, the impact of nonlinearity, even if present, on liquefaction prediction with the simplified procedure is diminished at higher levels of shaking. This is because most of the sandy fill in the study area that is susceptible to liquefaction is predicted with the simplified procedure to liquefy when PGA reaches approximately 0.4 g during a M7.8 earthquake, i.e., the liquefaction resistance boundary at $PGA \approx 0.4$ g reaches a nearly vertical asymptote at a corrected CPT tip resistance (q_{c1N}) of 160 (e.g., see Youd et al. 2001, Figure 4). Accordingly, most of the sand with $q_{c1N} < 160$ is predicted to liquefy, and sand with $q_{c1N} > 160$ is considered by the procedure to be too dense to liquefy. This explains why liquefaction probability in Figure 4 approaches an asymptote at ~ 0.4 g. Thus the impact of soil nonlinearity on predicted liquefaction probabilities may not be great at $PGA > 0.4$ g.

ACKNOWLEDGMENTS

We thank John Boatwright and David M. Boore for their counsel on predicting ground motions, and Glenn J. Rix for discussions about curve fitting the relation between liquefaction probability and PGA. Reviews by David M. Boore, Glenn J. Rix, and John C. Tinsley, III greatly improved the manuscript. Robert C. Jachens provided the traces of the San Andreas Fault shown in Figure 1.

REFERENCES

- Abrahamson, N. A., and Silva, W. J., 1997. Equations for estimating horizontal response spectra and peak acceleration from Western North America earthquakes: A summary of recent work, *Seismol. Res. Lett.* **68** (1), 128–153.
- Boatwright, J., and Bundock, H., 2005. Modified Mercalli Intensity maps for the 1906 San Francisco earthquake plotted in ShakeMap format, *U.S. Geol. Surv. Open-File Rep. 2005-1135* (<http://pubs.usgs.gov/of/2005/1135/>).
- Boore, D. M., 2005. Erratum: Equations for estimating horizontal response spectra and peak acceleration from western North American earthquakes: A summary of recent work, *Seismol. Res. Lett.* **76** (3), 368–369.
- Boore, D. M., Joyner, W. B., and Fumal, T. E., 1997. Empirical near-source attenuation relations for horizontal and vertical components of peak ground acceleration, peak ground velocity, and pseudo-absolute acceleration response spectra, *Seismol. Res. Lett.* **68** (1), 154–179.
- Brady, A. G., and Shakal, A. F., 1998. Strong-motion recordings, in *The Loma Prieta, California, Earthquake of October 17, 1989—Strong Ground Motion*, edited by R. D. Borcherdt, *U.S. Geol. Surv. Prof. Pap. 1551-A*, pp. A9–A38.
- Choi, Y., and Stewart, J. P., 2005. Nonlinear site amplification as function of 30 m shear wave velocity, *Earthquake Spectra* **21** (1), 1–30.
- Hamada, M., Isoyama, R., and Wakamatsu, K., 1995. *The 1995 Hyogoken-Nanbu (Kobe)*

- Earthquake—Liquefaction, Ground Displacement, and Soil Condition in the Hanshin Area*, The School of Science and Engineering, Waseda University, Tokyo, 194 pp.
- Hamada, M., and Wakamatsu, K., 1995. Liquefaction, ground deformation, and their caused damage to structure, *The 1995 Hyogoken-Nanbu Earthquake—Investigation into Damage To Civil Engineering Structures*, edited by M. Hamada, T. Ohmachi, and N. Ohbo, Japan Society of Civil Engineers, pp. 45–92.
- Helley, E. J., and Graymer, R. W., 1997. Quaternary Geology of Alameda County, and Parts of Contra Costa, Santa Clara, San Mateo, San Francisco, Stanislaus, and San Joaquin Counties, California, A Digital Database, *U.S. Geol. Surv. Open-File Rep. 97-97* (<http://wrgis.wr.usgs.gov/open-file/of97-97/>).
- Holzer, T. L., ed., 1998a. The Loma Prieta, California, earthquake of October 17, 1989—Liquefaction, *U.S. Geol. Surv. Prof. Pap. 1551-B*, 314 pp.
- Holzer, T. L., 1998b. Introduction, The Loma Prieta, California, earthquake of October 17, 1989—Liquefaction, edited by T. L. Holzer, *U.S. Geol. Surv. Prof. Pap. 1551-B*, pp. B1–B8.
- Holzer, T. L., Bennett, M. J., Noce, T. E., Padovani, A. C., and Tinsley, J. C., III, 2002. Liquefaction Hazard and Shaking Amplification Maps of Alameda, Berkeley, Emeryville, Oakland, and Piedmont: A Digital Database, *U.S. Geol. Surv. Open-File Rep. 02-296* (<http://geopubs.wr.usgs.gov/open-file/of02-296>).
- Holzer, T. L., Bennett, M. J., Noce, T. E., Padovani, A. C., and Tinsley, J. C., III, 2006. Liquefaction hazard mapping with LPI in the greater Oakland, California, area, *Earthquake Spectra* **22** (3), in press.
- Holzer, T. L., Bennett, M. J., Noce, T. E., and Tinsley, J. C., III, 2005b. Shear-wave velocity of surficial geologic sediments in Northern California: Statistical distributions and depth dependence, *Earthquake Spectra* **21** (1), 161–177.
- Holzer, T. L., Padovani, A. C., Bennett, M. J., Noce, T. E., and Tinsley, J. C., III, 2005a. Mapping NEHRP V_{S30} site classes, *Earthquake Spectra* **21** (2), 353–370.
- Idriss, I. M., 1990. Response of soft soil sites during earthquakes, *Proceedings, H. Bolton Seed Memorial Symposium*, edited by J. M. Duncan, BiTech Publishers, Vancouver, B.C., Canada, pp. 273–289.
- Idriss, I. M., 1993. Procedures for Selecting Earthquake Ground Motions at Rock Sites, Structural Division of the Building and Fires Research Lab, National Institute of Standards and Technology *NIST GCR 93-625*, Gaithersburg, MD, 7 pp.
- Iwasaki, T., Tatsuoka, F., Tokida, K.-I., and Yasuda, S., 1978. A practical method for assessing soil liquefaction potential based on case studies at various sites, *Proceedings, 2nd International Conference on Microzonation, San Francisco, Calif.*, pp. 885–896.
- Iwasaki, T., Tokida, K., Tatsuoka, F., Watanabe, S., Yasuda, S., and Sato, H., 1982. Microzonation for soil liquefaction potential using simplified methods, *Proceedings, 3rd International Earthquake Microzonation Conference*, Seattle, pp. 1319–1330.
- Joyner, W. B., and Boore, D. M., 1988. Measurement, characterization, and prediction of strong ground motion, Recent advances in ground-motion evaluation, in *ASCE Geotechnical Special Publication No. 20*, edited by J. L. Von Thun, New York, pp. 43–102.
- Robertson, P. K., and Wride, C. E., 1997. Cyclic liquefaction and its evaluation based on the SPT and CPT, *Proceedings, Evaluation of Liquefaction Resistance of Soils*, edited by T. L.

- Youd and I. M. Idriss, National Center for Earthquake Engineering Research Tech. Rep. *NCEER-97-0022*, pp. 41–87.
- Rogers, J. D., and Figuers, S. H., 1991. Site stratigraphy and near-shore development effects on soil amplification in the greater Oakland area, in *Loma Prieta Earthquake—Engineering Geology Perspectives*, edited by J. E. Baldwin, II, and N. Sitar, Association of Engineering Geologists, pp. 123–149.
- Seed, H. B., and Idriss, I. M., 1971. Simplified procedure for evaluating soil liquefaction potential, *J. Soil Mech. Found. Div.* **97** (9), 1249–1273.
- Seed, H. B., Tokimatsu, K., Harder, L. F., and Chung, R. M., 1985. Influence of SPT procedures in soil liquefaction resistance evaluations, *J. Geotech. Eng.* **111** (12), 1425–1445.
- Tinsley, J. C., III, Egan, J. A., Kayen, R. E., Bennett, M. J., Kropp, A., and Holzer, T. L., 1998. Appendix: Maps and descriptions of liquefaction and associated effects, in *The Loma Prieta, California, Earthquake of October 17, 1989—Liquefaction*, edited by T. L. Holzer, *U.S. Geol. Surv. Prof. Pap. 1551-B*, pp. B287–B314.
- Toprak, S., and Holzer, T. L., 2003. Liquefaction potential index: Field assessment, *J. Geotech. Geoenviron. Eng.* **129** (4), 315–322.
- U.S. Department of Commerce (USDC, 1959. Future Development of the San Francisco Bay Area 1960-2020, U.S. Office of Area Development, written for the U.S. Army Engineer District, San Francisco Corps of Engineers, 94 pp.
- U.S. Geological Survey (USGS, 2003. Is a Powerful Quake Likely to Strike in the Next 30 Years? *U.S. Geol. Surv. Fact Sheet 039-03*. <http://geopubs.wr.usgs.gov/fact-sheet/fs039-03>
- Working Group on California Earthquake Probabilities (WGCEP), 2003. Earthquake Probabilities in the San Francisco Bay Region: 2002–2031, *U.S. Geol. Surv. Open-File Rep. 03-214*. <http://geopubs.wr.usgs.gov/open-file/of03-214>
- Wald, D. A., Quitoriano, V., Heaton, T. H., and Kanamori, H., 1999. Relationship between peak ground acceleration, peak ground velocity, and Modified Mercalli Intensity in California, *Earthquake Spectra* **15** (3), 557–564.
- Youd, T. L., and Hoose, S. N., 1978. Historic Ground Failures in Northern California Triggered by Earthquakes, *U.S. Geol. Surv. Prof. Pap. 993*, 177 pp.
- Youd, T. L., and Idriss, I. M., Andrus, R. D., Arango, I., Castro, G., Christian, J. T., Dobry, R., Finn, W. D. L., Harder, L. F., Jr., Hynes, M. E., Ishihara, K., Koester, J. P., Liao, S. S. C., Marcuson, W. F., III, Martin, G. R., Mitchell, J. K., Moriwaki, Y., Power, M. S., Robertson, P. K., Seed, R. B., and Stokoe, K. H., II, 2001. Liquefaction resistance of soils: Summary report from the 1996 NCEER and 1998 NCEER/NSF workshops on evaluation of liquefaction resistance of soils, *J. Geotech. Geoenviron. Eng.* **127** (10), 817–833.

(Received 9 August 2006; accepted 1 November 2006)